Journal of Applied Mechanics and Technical Physics, Vol. 41, No. 2, 2000

MECHANISM OF SUPERDEEP PENETRATION OF PARTICLES INTO A METAL TARGET

S. P. Kiselev and V. P. Kiselev

UDC 534.2

A physicomathematical model of superdeep penetration taking into account the strength properties of the target is proposed. Based on this model, the problem of superdeep penetration of tungsten particles into a steel target has been solved for the first time.

The phenomenon of superdeep penetration of microparticles into metal targets was found in early 1980s [1] and described in detail in experimental papers, which are briefly reviewed, for example, in [2]. There are several different hypotheses for the mechanism of this phenomenon [2–7], but a comprehensive description is still lacking, which makes the construction of a full mathematical model of this phenomenon a timely problem.

The essence of the phenomenon of superdeep penetration of particles in a target is as follows. Let there be a metal target experiencing the action of a high-velocity flow of particles. Under certain conditions, a small fraction of particles (about 0.1%) penetrate to a great depth of hundreds and thousands of particle diameters. (Normally, the penetration depth is less than ten particle diameters.) Superdeep penetration is observed for particles whose diameter is $d \leqslant 100$ μm, the strength of the particles should be greater than the strength of the target, the particle velocity is $v_p \geqslant 10^3$ m/sec, and the mean free-stream density of the particles is $\rho_2 \geqslant 10^3$ kg/m^3.

Tungsten particles were usually used in experiments, and the target material was steel. An analysis of the steel target after the action of a flux of particles shows [8] that the channels behind the particles that penetrated to large depths $l \sim 10^3 d$ were completely collapsed. It is noted [8] that three qualitatively different regions can be distinguished in the vicinity of the axis of each collapsed channel. In the first region $r < 0.15d$, the material has completely lost its crystalline structure and is mixed with the particle material (r is the distance from the channel centerline). In the second region $0.15d \leqslant r \leqslant (0.5\text{–}1.0)d$, the target material has experienced an intense plastic deformation. In the third region $r \geqslant (0.5\text{–}1.0)d$, a weak plastic deformation of the material is observed. A physicomathematical model reflecting the above-described structure of material deformation is proposed in the present paper.

It was assumed [2–4] that the target material flow can be described within the framework of the perfect liquid model. In this case, the d'Alembert paradox is valid for an attached flow, and the force acting on the particle from the side of the material equals zero. The penetration depth is equal to the product of the particle velocity and the time t^* of existence of the pressure p in the target, which is responsible for collapse of the channel behind the particle. Since the pressure is generated by deceleration of particles in the surface layer, t^* is equal to the time of action of the particle flux on the target. A criterion of implementation of this regime is obtained from the condition of appearance of a jet catching up with the particle and pushing it, which is formed upon channel collapsing. This criterion has the form $p > \rho_s v_p^2 \tan^2 \alpha_*/2$, where ρ_s is the density of the target material and $\alpha_* \approx 20°$ is the critical angle of convergence of the jets at which a jet

Institute of Theoretical and Applied Mechanics, Siberian Division, Russian Academy of Sciences, Novosibirsk 630090. Translated from Prikladnaya Mekhanika i Tekhnicheskaya Fizika, Vol. 41, No. 2, pp. 37–46, March–April, 2000. Original article submitted March 29, 1999.

0021-8944/00/4102-0235 $25.00

catching up with the particle appears.

It should be noted that modeling of the target material by a perfect incompressible liquid is rather rough and contradicts the above-described structure of the channel behind the particle [8]. We show that the loss of strength of the material and its modeling by a liquid is possible only in the vicinity of the particle at distances not exceeding the particle diameter. In the remaining zone, the strains are small, and the material experiences elastoplastic deformations. The strain rates near the particle are large ($\dot{\varepsilon}_0 \sim v_p/d \sim 10^7$–$10^8$ sec^{-1}), and there is not enough time for heat removal from the slip surfaces, which leads to loss of strength of the material [9]. Denoting the mean distance between the planes where the deformation is localized as Δ, we write the condition of loss of strength as the inequality $\Delta^2/æ > d/v_p$, where $\Delta^2/æ$ is the time of temperature relaxation due to thermal conductivity and $æ$ is the thermal diffusivity. The magnitude of Δ should be of the order of the distance between the slip surfaces 0.1–1.0 μm. Substituting the values $\Delta \simeq 1.4$ μm, $æ = 2 \cdot 10^{-5}$ m^2/sec, and $v_p \simeq 10^3$ m/sec into this inequality, we obtain the restriction on the particle diameter $d \leqslant \Delta^2 v_p/æ \approx 100$ μm, which agrees with a similar estimate in [2, 3].

Assuming the velocity field in the vicinity of the particle to be described by the solution of the equation for a perfect liquid, in a spherical coordinate system we have $v_r = v_p(1 - (a/r)^3)\cos\theta$ and $v_\theta = -v_p(1 + (1/2)(a/r)^3)\sin\theta$ [10], where θ is the angle between the radius-vector and the velocity vector of the particle. Using these formulas, we find that the strain rate $\dot{\varepsilon} \sim \partial v_\theta/\partial r$ decreases with increasing radius r as a power-law function $\dot{\varepsilon}/\dot{\varepsilon}_0 = (a/r)^4$, where $a = d/2$ is the particle radius and $\dot{\varepsilon}_0 \sim v_p/d$ is the strain rate on the particle surface. It follows from this formula that the strain rate for $r = 3a$ is $\dot{\varepsilon} = \dot{\varepsilon}_0 \cdot 10^{-2} \sim 10^5$–$10^6$ sec^{-1}. For this strain rate, the loss of strength does not occur and the material retains its strength properties [11]. Thus, the radius of the zone of loss of strength $r \approx 3a$ has the order of the radius of the region of strong deformation observed in channels behind the particles [8]. This allows one to assume that the loss of strength of the material in the course of particle penetration occurs in the region of intense deformation $r \leqslant 3a$, and the material preserves its strength properties in the region of weak deformation $r \geqslant 3a$. Despite the fact that the mechanical properties of the material with loss of strength are similar to liquid properties, the material does not melt. The loss of strength of the material, in contrast to melting, requires low energy losses. For example, the melting of steel in a cylinder of diameter $0.3d$ and length $10^3 d$ requires the energy $E \approx 0.5$ J, which is two orders of magnitude greater than the kinetic energy of a tungsten particle with velocity $v_p = 10^3$ m/sec, density $\rho_p = 2 \cdot 10^4$ kg/m^3, and diameter $d = 100$ μm. Therefore, the loss of strength rather than melting of the material occurs near the channel axis $r < 0.15d$. Violation of the crystalline structure of the material is apparently related to a significant deformation, which arises due to viscous stresses and, according to Panin et al. [12], is accompanied by large local turnings.

We obtain a criterion of superdeep penetration taking into account the strength properties of the target material. We consider a solid spherical particle of diameter d moving in the target material along the x axis for the case where the material in the vicinity of the particle has lost strength. Let the particle have a velocity v_p and a coordinate x_p at the time t. During the time $\Delta t \approx d/v_p$, the particle shifts to the point $x_p' = x_p + d$. Then a spherical cavity (pore) of radius $a = d/2$ appears at the point x_p. Under the action of the pressure p, this pore is filled by the target material. If the pore is closed during the time Δt, an attached flow around the particle is observed. This leads to a dramatic decrease in the drag force and to superdeep penetration of the particle. It does not seem possible to construct an analytical solution that describes the flow of a viscoelastoplastic material in the vicinity of the particle.

To find the pore-collapse time τ, we consider the following model problem. We have a spherical cell of radius b with a pore of radius $a = d/2$ in the center of this cell. The pore radius coincides with the particle radius (Fig. 1). We assume the material to be in a liquid state in the layer $a < r < r_p$ and in a viscoplastic state in the layer $r_p < r < b$. For $a < r < r_p$, the liquid state models the loss of strength of the material, and the material preserves its strength properties in the layer $r_p < r < b$. Based on the above-derived estimate for the radius of the zone of material softening, we choose the upper boundary of the liquid layer $r_p = d$.

Since Andilevko et al. [8] do not give the upper boundary of the weakly deformed region, we have to

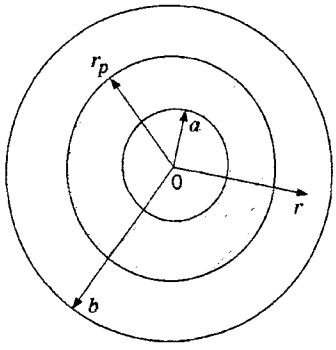

Fig. 1

involve additional considerations to determine b. Using the Hooke's law in a differential form $\dot{S}_{ij} = 2\mu\dot{e}_{ij}$ and the above-derived estimate for the strain rate $\dot{\varepsilon} \sim (v_p/d)(a/r)^4$, we evaluate the stresses arising at a point located at a distance r from the center of the particle:

$$S_{ij} \sim 2\mu\dot{\varepsilon}\Delta t \sim 2\mu\,\frac{v_p}{d}\Big(\frac{a}{r}\Big)^4\frac{d}{v_p} \sim 2\mu\Big(\frac{a}{r}\Big)^4.$$

Here $\Delta t = d/v_p$ is the characteristic time of deformation, S_{ij} and e_{ij} are the deviators of stress and strain tensors, and μ is the shear modulus. The stress at the boundary separating the elastic and plastic zones reaches the yield strength $S_{ij} \approx Y$. Substituting this value into the formula for S_{ij}, taking into account that $Y = 1$ GPa and $\mu = 80$ GPa for steel, we estimate the radius of the plastic zone as $r \sim 3.56a$. Assuming that the cell radius is equal to the plastic zone radius, we find $b = 2d$.

If we apply the pressure p to the external boundary of the cell, the pore collapses during a certain time τ. Ignoring the compressibility of the material, we write the equations that describe the spherically symmetric collapse of the pore [13]:

$$\rho_s\Big(\frac{\partial v_r}{\partial t} + v_r\frac{\partial v_r}{\partial r}\Big) = \frac{\partial\sigma_r}{\partial r} + 2\,\frac{\sigma_r - \sigma_\theta}{r}, \qquad \frac{\partial r^2 v_r}{\partial r} = 0,$$

$$\sigma_r - \sigma_\theta = 2\eta_0\Big(\frac{\partial v_r}{\partial r} - \frac{v_r}{r}\Big) \quad \text{for} \quad a < r < r_p, \tag{1}$$

$$\sigma_r - \sigma_\theta = Y + 2\eta\Big(\frac{\partial v_r}{\partial r} - \frac{v_r}{r}\Big) \quad \text{for} \quad r_p < r < b.$$

Here v_r is the velocity of motion of the material over the radius, σ_r and σ_θ are the components of the stress tensor in the spherical coordinate system (Fig. 1), η and Y are the viscosity and yield strength of the viscoplastic material, and η_0 is the viscosity of the liquid.

Integrating Eqs. (1) with respect to r with the boundary conditions

$$\sigma_r(a) = 0, \quad \sigma_r(b) = -p, \quad \sigma_r(r_p - 0) = \sigma_r(r_p + 0), \quad v_r(r_p - 0) = v_r(r_p + 0),$$

we obtain

$$p = \frac{2}{3}\,Y\,\ln\frac{\alpha}{\delta + \alpha - 1} + \frac{\rho_s a_0^2}{3(\alpha_0 - 1)^{2/3}}\Big(\ddot{\alpha}\Big(\frac{1}{\alpha^{1/3}} - \frac{1}{(\alpha - 1)^{1/3}}\Big) + \frac{\dot{\alpha}^2}{6}\Big(\frac{1}{(\alpha - 1)^{4/3}} - \frac{1}{\alpha^{4/3}}\Big)\Big)$$

$$- \frac{4}{3}\,\dot{\alpha}\Big(\frac{\eta - \eta_0}{\delta + \alpha - 1} - \frac{\eta}{\alpha} + \frac{\eta_0}{\alpha - 1}\Big), \tag{2}$$

$$v_r = \frac{a_0^3\dot{\alpha}}{3(\alpha_0 - 1)r^2}, \quad \alpha = \frac{b^3}{b^3 - a^3} = \frac{b^3}{b_0^3 - a_0^3}, \quad \delta = \frac{r_p^3 - a^3}{b^3 - a^3},$$

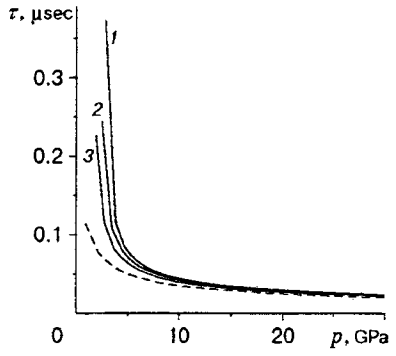

Fig. 2

where $\alpha_0 = \alpha(0)$, $a_0 = a(0) = d/2$, $b_0 = b(0) = 2d$, the dots denote derivatives with respect to time, and δ is the fraction of the liquid material in the cell. Assuming $\dot{\alpha} = \ddot{\alpha} = 0$ and $\alpha = 1$ in the first equation of system (2), we find the minimum pressure p_* for which a complete collapse of the pore occurs:

$$p_* = (2/3)Y \ln(1/\delta).$$

It follows from here that, if the material does not lose its strength, we have $\delta \to 0$ and $p_* \to \infty$, and the pore does not collapse at all. A hollow channel is formed behind the particle, and superdeep penetration becomes impossible. In our case, for steel with $\delta \approx 0.11$ and $Y = 1.2$ GPa we obtain the minimum pressure $p_* \simeq 1.4$ GPa. From Eqs. (2), it follows that the time of the complete collapse of the pore τ is the function

$$\tau = \psi(p, \rho_s, a_0, \eta, Y, \alpha_0, \delta). \tag{3}$$

[Since $\eta \gg \eta_0$, we ignore the dependence on η_0 in writing Eq. (3)]. Using the π-theorem, we can rewrite formula (3) in the dimensionless form

$$\tau = a_0 \sqrt{\frac{2\rho_s}{p}}\, \varphi\left(\alpha_0, \delta, \frac{p}{Y}, \frac{\sqrt{\rho_s p}\, a_0}{\eta}\right). \tag{4}$$

The function φ in Eq. (4) was found by numerical integration of system (2).

It is noted above that the material should lose its strength in the vicinity of the particle in the case of superdeep penetration, and the pore arising behind the particle should collapse during the time $\Delta t = d/v_p$. Hence, the condition of superdeep penetration can be written in the form of the inequalities

$$\tau \leqslant d/v_p \leqslant \Delta^2/æ. \tag{5}$$

Using formula (4), we recast the first inequality of system (5) as follows:

$$p \geqslant \frac{\rho_s v_p^2}{2} \varphi^2. \tag{6}$$

From comparison of formula (6) with the criterion obtained in [2–4], it follows that the quantity φ in these papers is a constant $\varphi = \tan \alpha_*$, whereas in the proposed model φ depends on the viscous and strength properties of the material and on the cell parameters [see formula (4)]. Figure 2 shows the collapse time τ versus the pressure p obtained by numerical integration of Eq. (2) for the following parameters: $\rho_s = 7.85 \cdot 10^3$ kg/m^3, $Y = 1.2$ GPa, $\eta = 10^2$ Pa $\cdot$ sec, $\eta_0 = 2 \cdot 10^{-3}$ Pa $\cdot$ sec, $a_0 = 50$ μm, and $r_p = 100$ μm. The dashed curve describes the dependence of τ on p for a liquid cell $Y = 0$, $\eta = \eta_0$ for $b_0 = 200$ μm. The solid curves 1–3 describe the dependences $\tau(p)$ with account of strength $Y = 1.2$ GPa for initial radii of the cell $b_0 = 300$, 250, and 200 μm. The cell radius b_0 has a weak effect on the collapse time. Taking into account the material strength $Y \neq 0$ leads to a significant increase in τ for pressures $p < 5$ GPa.

The force acting on the particle from the target can be determined from the formula proposed by Zlatin [14]

$$\boldsymbol{F} = -\Big(H + p + \frac{\rho_s}{2}(\boldsymbol{v}_p - \boldsymbol{v}_1)^2\Big)\frac{\pi d^2}{4}\frac{\boldsymbol{v}_p - \boldsymbol{v}_1}{|\boldsymbol{v}_p - \boldsymbol{v}_1|}, \tag{7}$$

where $\boldsymbol{v}_1$ is the velocity of the target material. The first term in brackets H, called the dynamic hardness, is caused by the work of hardness forces during material deformation. If the particle penetrates into the material at the length l, the work of these forces is $A = \int \rho_s \Delta E\, dV$. The volume of integration is a cylindrical channel behind the particle of radius d and length l; therefore, we have $A \approx \rho_s \Delta E \pi d^2 l$. The increase in the specific energy ΔE is estimated from the formula

$$\Delta E = \int \frac{1}{\rho_s}\sigma_{ij}\dot{\varepsilon}_{ij}\, dt \approx \frac{1}{\rho_s} S_{ij}\dot{e}_{ij}\Delta t \approx \frac{1}{\rho_s} Y \frac{v_p}{d}\frac{d}{v_p} \approx \frac{Y}{\rho_s},$$

where $S_{ij} \sim Y$, $\dot{e}_{ij} \sim v_p/d$, $\Delta t \approx d/v_p$, and $\sigma_{ij} = -p\delta_{ij} + S_{ij}$ is the stress tensor.

Substituting ΔE into the formula for work, we have $A \approx \pi d^2 l Y$. Simultaneously, the work is found from the formula $A = (\pi d^2/4) l H$. Equating these two expressions, we obtain $H \approx 4Y$, which is twice as large as the experimentally determined hardness of steel $H = 2$ GPa [14]. It follows from this reasoning that $H \approx 0$ if the material loses its strength in the vicinity of the particle within $r < d$.

The second and third terms in brackets in formula (7) are caused by formation of a cavity behind the particle. In this case, the pressure acting on the first hemisphere of the particle $p + \rho_s(\boldsymbol{v}_p - \boldsymbol{v}_1)^2/2$ multiplied by the mid-section area $\pi d^2/4$ determines the force acting on the particle. If the regime of attached flow is observed, there is no cavity behind the particle, and this force is equal to zero. In the case of superdeep penetration, both conditions (5) are fulfilled, and the right side in Eq. (7) vanishes. It is necessary to take into account, however, that plastic deformations of the material with the strain rate $\dot{\varepsilon} \sim (v_p/d)(a/r)^4 \sim 10^{-2} v_p/d$ occur outside the zone of material softening $d < r < 2d$. This decreases the work of the strength forces and, hence, the dynamic hardness $H' \approx 10^{-2} H$ by two orders of magnitude. Taking into account the strength properties of the target material leads to even smaller values of $\dot{\varepsilon}$; therefore, the inequality $H' \leqslant 10^{-2} H$ is valid in this case for dynamic hardness.

In the zone of material softening $d/2 < r < d$, the yield strength is $Y = 0$, and the viscosity coincides with the melt viscosity $\eta_0 = 2 \cdot 10^{-3}$ Pa · sec. Correspondingly, the Reynolds number for the flow parameters around the particle $v_p \approx 10^3$ m/sec, $d \approx 100$ μm, and $\rho_s = 8 \cdot 10^3$ kg/m^3 is $\mathrm{Re} = \rho_s v_p d/\eta_0 \approx 4 \cdot 10^5$. Hence, viscous forces are manifested only in a thin boundary layer of thickness $\delta \approx 5.6\sqrt{\nu_0 d/v_p} \approx 5.6 d/\sqrt{\mathrm{Re}} \approx 1$ μm, where $\nu_0 = \eta_0/\rho_s$ [10]. Apparently, the first region of intense deformation in the channel of diameter about $0.3d$ observed experimentally [8] is the boundary layer separating from the particle. Nevertheless, the diameter of this region is 30 μm for $d \approx 100$ μm, which is greater than the above estimate of δ by an order of magnitude. This difference may be caused by the fact that the strain rate and temperature in the boundary layer decrease after its detachment from the particle. This leads to a dramatic increase in viscosity and the boundary-layer thickness in the channel behind the particle. Since $\delta \ll d$, the force of viscous drag of the particle can be determined using the self-similar Blasius solution. Multiplying the viscous stress tensor in the plate [10] by the particle-surface area, we obtain

$$F'_\eta = \frac{1}{2}\rho_s v_p^2 \frac{1.3}{\sqrt{\mathrm{Re}}}\pi d^2.$$

As a result, the total force acting on the particle in the superdeep penetration regime is

$$\boldsymbol{F}_p = -\left(H' + 2.6\frac{\rho_s(\boldsymbol{v}_p - \boldsymbol{v}_1)^2}{\sqrt{\mathrm{Re}}}\right)\frac{\pi d^2}{4}\frac{\boldsymbol{v}_p - \boldsymbol{v}_1}{|\boldsymbol{v}_p - \boldsymbol{v}_1|}, \tag{8}$$

where $\mathrm{Re} = |\boldsymbol{v}_p - \boldsymbol{v}_1|\, d/\nu_0$.

As noted above, only a very small fraction of incident particles (about 0.1%) penetrates to a large depth. This may be caused by the screening effect of the incident particles by those particles that are accumulated in the surface layer of the target after a certain time t. If the volume concentration of particles m_2 in the surface layer is smaller that some critical value m_2^*, the particles falling on the surface can penetrate into the metal. (The volume concentration of particles m_2 is the fraction of unit volume occupied by the particles.)

If $m_2 > m_2^*$, the incident particle collides with the particles in the surface layer and is stuck in it. Individual impulses generated by the incident particles are distributed among all particles of the layer. As a result, a dense layer of particles acts on the target with the mean pressure [2] $p_L = 0.3\rho_L v_L c$, where c is the mean velocity of sound in the target and ρ_L and v_L are the mean particle density and velocity in the cloud. Hence, the particles penetrate into the target under the condition

$$\langle m_2 \rangle < m_2^*, \tag{9}$$

where $\langle m_2 \rangle = \int_0^{l_p} m_2\, dx/l_p$ is the mean volume concentration of particles in the surface layer of thickness l_p (l_p is the velocity-relaxation length during particle penetration into the material). Let us derive a formula for l_p. Substituting the force $\boldsymbol{F}_p$ from formula (7) into the equation of particle motion and ignoring the pressure and dynamic hardness, we obtain the equation of motion $dv_p/dt = -v_p^2/l_p$, which incorporates the velocity-relaxation length $l_p = 4\rho_p d/\rho_s$. The value of m_2^* was chosen by matching the numerical and experimental results in terms of the number of penetrated particles $m_2^* = 0.25$.

We formulate the equations that describe the process of superdeep penetration of the particles. As noted above, the particle strength is always greater than the target-material strength; therefore, the particles can be considered as incompressible spheres of diameter d. The volume concentration of the particles penetrating into the target is low ($m_2 \ll 1$), and the collisions between the particles can be ignored. To describe the motion of the particles and the target material, we use the continuum-discrete model developed previously for a gas–particle mixture [13]. In this model, the particles are described by the collision-free kinetic equation

$$\frac{\partial f}{\partial t} + \boldsymbol{v}_p \frac{\partial f}{\partial \boldsymbol{x}} + \frac{\partial}{\partial \boldsymbol{v}_p}\Big(\frac{\boldsymbol{F}_p}{m_p} f\Big) = 0, \quad m_2 = \frac{\pi d^3}{6}\int f\, dV_v, \quad \langle \boldsymbol{v}_p \rangle = \frac{\pi d^3}{6m_2}\int \boldsymbol{v}_p f\, dV_v, \tag{10}$$

where $f = f(t, \boldsymbol{v}_p, \boldsymbol{x})$ is a single-particle distribution function, $dV_v = dv_{px}\, dv_{py}\, dv_{pz}$ is the infinitesimal volume in the space of particle velocities, $m_p = \pi d^3 \rho_p/6$ is the particle mass, and $\langle \boldsymbol{v}_p \rangle$ is the mean velocity of the particles. The force $\boldsymbol{F}_p$ is found from formulas (7) and (8) and depends on the regime of particle motion.

System (10) should be supplemented by equations for the target material. Using tensor notation, we write them in the coordinate system x^i with the basis vectors $\boldsymbol{e}_i$:

$$\frac{\partial \rho_s}{\partial t} + \nabla_i \rho_s v_{1i} = 0, \quad \rho_s \frac{dv_{1i}}{dt} = \nabla_j \sigma_{ij} - F_i, \quad \rho_s \frac{dE}{dt} = \sigma_{ij}\dot{\varepsilon}_{ij} + \dot{Q},$$

$$\frac{d}{dt} = \frac{\partial}{\partial t} + v_{1i}\nabla_i, \quad \sigma_{ij} = -p\delta_{ij} + S_{ij}, \quad \dot{\varepsilon}_{ij} = \frac{1}{2}(\nabla_i v_{1j} + \nabla_j v_{1i}),$$

$$\dot{e}_{ij} = \dot{\varepsilon}_{ij} - \frac{1}{3}\dot{\varepsilon}_{kk}\delta_{ij}, \quad \hat{S}_{ij} = \begin{cases} 2\mu\dot{e}_{ij}, & (3/2)S_{ij}S_{ij} < Y^2, \\ -\lambda S_{ij} + 2\mu\dot{e}_{ij}, & (3/2)S_{ij}S_{ij} = Y^2, \end{cases} \tag{11}$$

$$\hat{S}_{ij} = \frac{dS_{ij}}{dt} - \omega_{ik}S_{jk} - \omega_{jk}S_{ik}, \quad \omega_{ij} = \frac{1}{2}(\nabla_i v_{1j} - \nabla_j v_{1i}), \quad p = p_{\text{cold}} + p_{\text{therm}},$$

$$p_{\text{cold}} = K\Big(\frac{\rho_s}{\rho_s^0} - 1\Big), \quad E = E_{\text{cold}} + E_{\text{therm}}, \quad E_{\text{cold}} = \frac{K}{2\rho_s^0}\Big(\frac{1-\rho_s}{\rho_s^0}\Big)^2 + \frac{\mu}{\rho_s} e_{ij}^e e_{ij}^e,$$

$$e_{ij}^e = \frac{S_{ij}}{2\mu}, \qquad p_{\text{therm}} = \Gamma\rho_s E_{\text{therm}}, \qquad i, j = 1, 2, 3.$$

Here $\dot{e}_{ij}$, S_{ij}, $\dot{\varepsilon}_{ij}$, σ_{ij}, and ω_{ij} are the tensors of the deviator of the stress and strain rates, strain rate, stress, and turning (summation is performed over repeated indices), E, E_{cold}, and E_{therm} are the specific internal energy and its cold and thermal components, p, p_{cold}, and p_{therm} are the pressure and its cold and thermal components, and K and μ are the volume compression and shear moduli. The material is described by the

Hooke's law in the elastic zone and by the Prandtl–Reiss relations in the elastoplastic zone. The force $\boldsymbol{F}$ of interaction between the particles and material and the energy-dissipation rate $\dot{Q}$ are found from the formulas

$$\boldsymbol{F} = \int \boldsymbol{F}_p f \, dV_v, \qquad \dot{Q} = \int \boldsymbol{F}_p(\boldsymbol{v}_1 - \boldsymbol{v}_p) f \, dV_v, \tag{12}$$

where $\boldsymbol{F} = F_i \boldsymbol{e}_i$.

Using this model, we solved a one-dimensional problem of superdeep penetration of particles into the target. The target was a material layer of thickness h^0 with a particle flux incoming from the left. In the one-dimensional case, system (5), (7), (10)–(12) becomes much simpler and has the form

$$\frac{\partial f}{\partial t} + v_p \frac{\partial f}{\partial x} + \frac{\partial}{\partial v_p}\Big(\frac{F_p}{m_p} f\Big) = 0, \quad m_p = \frac{\pi d^3}{6}\rho_p, \quad m_2 = \frac{\pi d^3}{6}\int\limits_{-\infty}^{\infty} f \, dv_p,$$

$$\frac{\partial \rho_s}{\partial t} + \frac{\partial}{\partial x}\rho_s v_1 = 0, \quad \rho_s \frac{dv_1}{dt} = \frac{\partial \sigma_1}{\partial x} - F, \quad \rho_s \frac{dE}{dt} = \sigma_1 \dot{\varepsilon}_1 + \dot{Q}, \quad \frac{d}{dt} = \frac{\partial}{\partial t} + v_1 \frac{\partial}{\partial x},$$

$$\sigma_1 = S_1 - p, \qquad S_2 = S_3, \qquad S_1 + S_2 + S_3 = 0,$$

$$\dot{S}_i' = 2\mu \dot{e}_i, \quad S_i = \begin{cases} S_i', & \dfrac{2}{3}\displaystyle\sum_{i=1}^{3}(S_i')^2 < Y^2, \\ \sqrt{\frac{2}{3}} S_i' Y \Big/ \sqrt{\displaystyle\sum_{i=1}^{3}(S_i')^2}, & \dfrac{2}{3}\displaystyle\sum_{i=1}^{3}(S_i')^2 \geqslant Y^2, \end{cases} \tag{13}$$

$$p = p_{\text{cold}} + p_{\text{therm}}, \quad p_{\text{cold}} = K\Big(\frac{\rho_s}{\rho_s^0} - 1\Big), \quad E = E_{\text{cold}} + E_{\text{therm}}, \quad E_{\text{cold}} = \frac{1}{2\rho_s^0}\Big(K\Big(1 - \frac{\rho_s}{\rho_s^0}\Big)^2 + 3\mu(e_1^e)^2\Big),$$

$$\dot{e}_1^e = \frac{\dot{S}_1}{2\mu}, \quad p_{\text{therm}} = \Gamma \rho_s E_{\text{therm}}, \quad \dot{\varepsilon}_1 = \frac{\partial v_1}{\partial x}, \quad \dot{\varepsilon}_2 = \dot{\varepsilon}_3 = 0,$$

$$F = \int\limits_{-\infty}^{\infty} F_p f \, dv_p, \qquad \dot{Q} = \int\limits_{-\infty}^{\infty} F_p(v_1 - v_p) f \, dv_p,$$

$$F_p = \begin{cases} -\Big(H + p + \dfrac{\rho_s}{2}(v_p - v_1)^2\Big)\dfrac{\pi d^2}{4}\dfrac{v_p - v_1}{|v_p - v_1|}, \\ -\Big(H' + 2.6\dfrac{\rho_s (v_p - v_1)^2}{\sqrt{\mathrm{Re}}}\Big)\dfrac{\pi d^2}{4}\dfrac{v_p - v_1}{|v_p - v_1|}, \qquad \dfrac{æ}{\Delta^2} \leqslant \dfrac{|v_p - v_1|}{d} \leqslant \dfrac{1}{\tau}. \end{cases}$$

The first relation for the force F_p is used if the condition of superdeep penetration $æ/\Delta^2 \leqslant |v_p - v_1|/d \leqslant 1/\tau$ is not satisfied and at the stage where the penetration depth of the particles in the target is equal to the diameter d. If the strain rate $\dot{\varepsilon} = |v_p - v_1|/d$ satisfies the inequality $\dot{\varepsilon} > æ/\Delta^2$, then H' should be substituted for H in the first relation for F_p.

System (13) is valid in the region $x_L(t) < x < x_R(t)$ whose left $x_L(t)$ and right $x_R(t)$ boundaries change with time. As long as inequality (9) is satisfied, the particles penetrate into the target. In this case, the condition of zero stress $\sigma_1(x_L(t)) = 0$ and the flux of particles

$$j(x_L(t)) = \rho_L v_L$$

are prescribed at the left boundary $x_L(t)$. The free-stream velocity v_L and the mean density of particles ρ_L are found from the formulas

$$v_L = v_L^0 \exp(-\alpha_1 t/\tau_0), \qquad \rho_L = \rho_L^0 \exp(\alpha_2 t/\tau_0), \tag{14}$$

which were obtained by Andilevko et al. [15] by approximation of numerical results on powder acceleration by explosive energy. When inequality (9) becomes invalid, the incident particles are screened, and we set

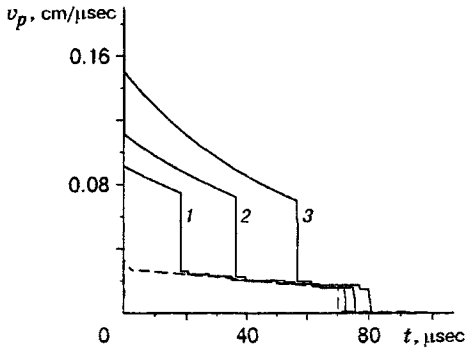

Fig. 3

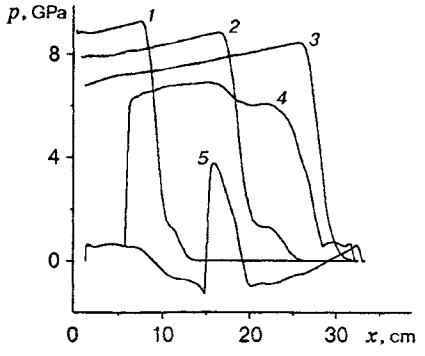

Fig. 4

$j(x_L(t)) = 0$ and $\sigma_1(x_L(t)) = -0.3\rho_L v_L c$, where ρ_L and v_L are found from formulas (14), at the boundary $x_L(t)$. The condition of zero stress $\sigma_1(x_R(t)) = 0$ is imposed at the right boundary. The target is assumed to be rather "thick" and the particles do not go outside the right boundary; therefore, no conditions are imposed on them at the right boundary. At the time $t = 0$, the velocity v_1, pressure p, and stresses σ_i are equal to zero, and the density is $\rho_s = \rho_s^0$.

System (13) was solved by the numerical method developed previously by the authors for calculation of gas–particle mixture flows and described in detail in [16]. The equations that describe the behavior of the target material were solved in Eulerian moving coordinates using the "cross" scheme [17]. The collision-free kinetic equation for the particles was solved in Lagrangian coordinates. The cloud of particles at the entrance to the material was divided into cells in such a way that the particles in this cell had equal velocities. In this case, the equations of motion of the cell $dx/dt = v_p$ and $dv_p/dt = F_p/m_p$ coincided with the characteristics of the kinetic equation. The material velocity, pressure, and density in particle cells were found by interpolation. The target material was steel with the parameters $\rho_s^0 = 7.85 \cdot 10^3$ kg/m^3, $\mu = 80$ GPa, $K = 160$ GPa, $Y = 1$ GPa, and $H = 2$ GPa. The tungsten particles had a diameter $d = 100$ μm and density $\rho_p = 19.8 \cdot 10^3$ kg/m^3. The dynamic hardness and viscosity of the material with the loss of strength were $H' = 2 \cdot 10^{-3}$ GPa and $\eta_0 = 10^{-3}$ Pa · sec. The parameters entering Eq. (14) were chosen similar to those in [2, 15]: $v_L^0 = 2$ km/sec, $\rho_L^0 = 3 \cdot 10^3$ kg/m^3, $\alpha_1 = 1.61$, $\alpha_2 = 0.92$, and $\tau_0 = 70$ μsec, where τ_0 is the time of loading of the target by the particle flux. The coordinates of the target boundaries at the initial time $t = 0$ were $x_L(0) = 0$ and $x_R(0) = 0.3$ m.

Figure 3 shows the velocity of three particle cells (in what follows, we will call them simply particles for brevity) versus the time t. The particles are incident onto the left boundary of the target at the times $t_1 = 0$, $t_2 = 0.19$ μsec, and $t_3 = 0.38$ μsec. During the time $\Delta t \approx 0.1$ μsec, the particles are strongly decelerated near the target boundary until they penetrate deeply into the target and the condition of superdeep penetration is fulfilled. At the second stage, the regime of superdeep penetration is attained, the force acting on the particles is small, and their velocity is slow. At the third stage, the condition of superdeep penetration (5) is no longer valid, the particles are drastically decelerated again, and their velocity decreases to the material velocity. The dashed curve in Fig. 3 shows the velocity of the left boundary of the target.

Figure 4 shows the pressure distributions in the target $p(x)$ for several times t from the beginning of penetration of the particles into the target with an interval $\Delta t = 20$ μsec. It follows from Fig. 3 that the termination of superdeep penetration is related to particle deceleration to the velocity $v_p \approx 750$ m/sec where condition (5) is no longer valid. As follows from Fig. 4, the mean pressure acting in the material at the time $t \approx 60$ μsec is still rather high ($p \approx 8$ GPa). Hence, the assumption of Al'tshuler et al. [2, 3] and Andilevko [4] that the time of superdeep penetration of particles equals the time of action of high pressure in the material for thick targets is incorrect. The later the particles enter the target, the less they are decelerated in the boundary zone. These particles overtake the particles that entered the target earlier and penetrate to great distances (see Fig. 3). The reason is that the first particles start to penetrate into the target when the

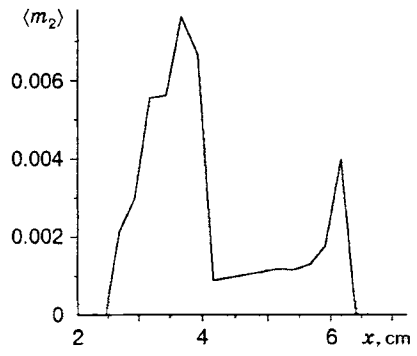

Fig. 5

pressure there equals zero, and they spend more energy for deceleration and generation of high pressure than the particles that entered the target at later times. This effect is the reason for a nonmonotonic distribution of the particle concentration depending on the penetration depth.

Figure 5 shows the dependence of the averaged volume concentration of particles $\langle m_2 \rangle$ on the x coordinate at the time $t = 100$ μsec. [The calculated dependence $m_2(x)$ had both regular and fluctuating components, the latter being related to the initial numerical discretization of the cloud into cells. As the particles penetrated into the material, the distance between them increased and the discreteness increased too. Fluctuations were eliminated by averaging the calculated value of $m_2(x)$ using the formula $\langle m_2 \rangle = \dfrac{1}{\Delta l} \displaystyle\int_{\Delta l} m_2(x)\, dx$; the value of Δl was chosen empirically and was equal to $25d$.] It follows from Fig. 5 that the particles penetrate to a maximum depth of the order of $500d$. The dependence $\langle m_2 \rangle(x)$ is nonmonotonic and has two maxima. The first maximum is located near the left boundary of the target and corresponds to the particles that spent their kinetic energy for pressure generation in the target. The second local maximum at $x \approx 6$ cm corresponds to the particles that enter the target at later times when there is a rather high pressure p in it. In this case, after penetration to the diameter d, the particles started to move in the regime of superdeep penetration, slowly losing their velocity. Note that the dependence $m_2(x)$ for tungsten particles obtained in the experiment [8] is also nonmonotonic and has two maxima: near the boundary and at a large depth ($x \approx 4.6$ cm).

Thus, a mathematical model used to solve the problem of superdeep penetration has been developed in the present paper. The calculation results for the penetration depth and distribution of the volume concentration of particles in the target are in qualitative agreement with experimental data.

REFERENCES

1. K. I. Kozorezov, V. N. Maksimenko, and S. M. Usherenko, "Effects of interaction of discrete microparticles with a solid body," in: *Selected Problems of Modern Mechanics* [in Russian], Part 1, Izd. Mosk. Univ. Publ., Moscow (1981), pp. 115–119.
2. L. V. Al'tshuler, S. K. Andilevko, G. S. Romanov, and S. M. Usherenko, "Treatment of a metal target by a flux of powdered particles. Superdeep penetration," *Inzh.-Fiz. Zh.*, **61**, No. 1, 41–45 (1991).
3. L. V. Al'tshuler, S. K. Andilevko, G. S. Romanov, and S. M. Usherenko, "Model of superdeep penetration," *Pis'ma Zh. Tekh. Fiz.*, **15**, No. 5, 55–57 (1989).
4. S. K. Andilevko, "Hydrodynamic model of superdeep penetration of absolutely rigid axisymmetric particles into a semi-infinite metal target," *Inzh.-Fiz. Zh.*, **71**, No. 3, 399–403 (1998).
5. S. S. Grigoryan, "Nature of 'superdeep' penetration of solid microparticles into solid materials," *Dokl. Akad. Nauk SSSR*, **292**, No. 6, 1319–1323 (1987).

6. G. G. Chernyi, "Mechanism of anomalously low drag upon motion of bodies in solid media," *ibid.*, pp. 1324–1328.
7. V. A. Simonenko, N. A. Skorkin, and V. V. Bashurov, "Penetration of individual microparticles into rigid barriers on collision of powder streams with them," *Fiz. Goreniya Vzryva*, **27**, No. 4, 46–51 (1991).
8. S. K. Andilevko, E. A. Doroshkevich, S. S. Karpenko, et al., "Variation of steel density upon superdeep penetration," *Inzh.-Fiz. Zh.*, **71**, No. 3, 394–398 (1998).
9. D. E. Grady and J. R. Asay, "Calculation of thermal trapping in shock deformation of aluminum," *J. Appl. Phys.*, **53**, No. 11, 7350–7356 (1982).
10. S. V. Vallander, *Lectures in Hydroaeromechanics* [in Russian], Izd. Leningrad. Univ., Leningrad (1978).
11. R. J. Clifton, "Dynamic plasticity," *Trans. ASME, Ser. E, J. Appl. Mech.*, **50**, No. 46, 941–952 (1983).
12. V. E. Panin, V. A. Likhachev, and Yu. V. Grinyaev, *Structural Levels of Deformation of Solids* [in Russian], Nauka, Novosibirsk (1985).
13. S. P. Kiselev, G. A. Ruev, A. P. Trunev, et al., *Shock-Wave Processes in Two-Component and Two-Phase Media* [in Russian], Nauka, Novosibirsk (1992).
14. N. A. Zlatin and G. I. Mishin (eds.), *Ballistic Facilities and Their Application in Experimental Studies* [in Russian], Nauka, Moscow (1974), pp. 194–205.
15. S. K. Andilevko, G. S. Romanov, and S. M. Usherenko, "Explosive accelerator of powdered particles with a cylindrical cavity filled by tungsten powder," *Inzh.-Fiz. Zh.*, **61**, No. 1, 46–51 (1991).
16. V. P. Kiselev, S. P. Kiselev, and V. M. Fomin, "Interaction of a shock wave with a cloud of particles of finite dimensions," *Prikl. Mekh. Tekh. Fiz.*, **35**, No. 2, 26–37 (1994).
17. M. L. Wilkins, "Calculation of elastoplastic flows," in: B. Alder, S. Fernbach, and M. Retenberg (eds.), *Methods of Computational Physics*, Vol. 3, Academic Press, New York (1964), pp. 212–263.